

Exploring the Boundaries of On-Device Inference: When Tiny Falls Short, Go Hierarchical

Adarsh Prasad Behera
IMDEA Networks Institute
Madrid, Spain
adarsh.behera@imdea.org

José Gallego
IMDEA Networks Institute
Madrid, Spain
jose.gallego@imdea.org

Paulius Daubaris
University of Helsinki
Helsinki, Finland
paulius.daubaris@helsinki.fi

Roberto Morabito
Eurecom
Biot, France
roberto.morabito@eurecom.fr

Iñaki Bravo
IMDEA Networks Institute
Madrid, Spain
inaki.bravo@imdea.org

Joerg Widmer
IMDEA Networks Institute
Madrid, Spain
joerg.widmer@imdea.org

Jaya Prakash Champati
IMDEA Networks Institute
Madrid, Spain
jaya.champati@imdea.org

ABSTRACT

On-device inference holds great potential for increased energy efficiency, responsiveness, and privacy in edge ML systems. However, due to less capable ML models that can be embedded in resource-limited devices, use cases are limited to simple inference tasks such as visual keyword spotting, gesture recognition, and predictive analytics. In this context, the Hierarchical Inference (HI) system has emerged as a promising solution that augments the capabilities of the local ML by offloading selected samples to an edge server/cloud for remote ML inference. Existing works demonstrate through simulation that HI improves accuracy. However, they do not account for the latency and energy consumption on the device, nor do they consider three key heterogeneous dimensions that characterize ML systems: hardware, network connectivity, and models.

In contrast, this paper systematically compares the performance of HI with on-device inference based on measurements of accuracy, latency, and energy for running embedded ML models on five devices with different capabilities and three image classification datasets. For a given accuracy requirement, the HI systems we designed achieved up to 73% lower latency and up to 77% lower device energy consumption than an on-device inference system. The key to building an efficient HI system is the availability of small-size, reasonably accurate on-device models whose outputs can be effectively differentiated for samples that require remote inference. Despite the performance gains, HI requires on-device inference for all samples, which adds a fixed overhead to its latency and energy consumption. Therefore, we design a hybrid system, Early Exit with HI (EE-HI), and demonstrate that compared to HI, EE-HI reduces the latency up to 59.7% and lowers the device’s energy consumption up to 60.4%.

1 INTRODUCTION

Deep Learning (DL) inference on data generated by *end devices* such as IoT sensors, smartphones, and drones enables significant improvements in operational efficiency and functionality across

various sectors, including industrial automation, smart cities, remote healthcare, smart agriculture, and other sectors. Performing DL inference locally on the device has the added advantage of increased energy efficiency [3], responsiveness, and privacy and holds great promise for real-time decision-making. Thus, significant efforts have been directed towards designing and developing compact DL models specifically tailored for deployment on end devices [6, 10, 30]. This resulted in a plethora of DL models, such as MobileNet [31], EfficientNet [33], and Gemma 2B large language model [8], which can be embedded on moderately powerful smartphones. Additionally, tinyML models like ResNet-8 [2] have been designed for extremely resource-limited micro-controller units (MCUs).

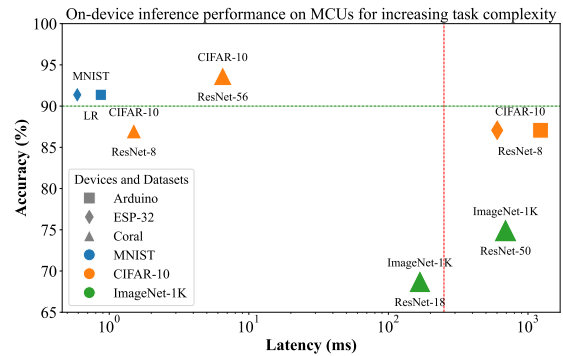


Figure 1: Measured inference accuracy and latency per inference for various models on different MCUs: Arduino Nano, ESP-32, and Coral Micro, for the MNIST, CIFAR-10, and ImageNet-1K datasets. As the inference complexity increases from MNIST to ImageNet-1K, even resorting to larger DL models and powerful MCU Coral Micro (with TPU) may be insufficient to satisfy QoS requirements; for example 90% accuracy (green line) and 250 ms response time (red line).

Especially when considering DL inference on MCUs, despite the advances in models’ optimizations and improvements, the end-product use cases of on-device inference are limited to applications involving simple inference tasks – visual keyword spotting on smartphones, gesture recognition on smart cameras, and predictive analytics for industrial machines on sensors [16]. We indeed argue that on-device inference becomes inadequate as the complexity of the inference tasks increases. For this purpose, consider an image classification application¹ with a QoS requirement of at least 90% accuracy and maximum 250 ms latency². In Fig. 1, we present the accuracy and latency for different ML models on three MCUs: Arduino Nano, ESP-32, and Coral Micro (cf. Table 1). Of the MCUs, Coral Micro is the most powerful, featuring a Tensor Processing Unit (TPU). For the inference tasks, we categorize MNIST image classification as a simple task, CIFAR-10 as a moderately complex task, and ImageNet-1K as a complex task. Observe that Arduino Nano and ESP-32 satisfy the QoS requirement for the MNIST dataset using Logistic Regression (LR). But both devices fall short of latency and accuracy requirements for CIFAR-10 dataset because running the state-of-the-art tinyML model ResNet-8, which has 87% accuracy, takes at least 600 ms. Coral Micro can meet the QoS requirements for CIFAR-10, using a bigger DL model ResNet-56, but it cannot do so for ImageNet-1K.

The issues discussed above hinder the large-scale adoption of on-device inference. An alternate solution for devices connected to a network is to use an edge server/cloud that uses a state-of-the-art large-size DL model. By offloading all the samples for *remote inference* on the large-size DL model, a device can achieve higher accuracy rather than inferring locally. However, fully offloading ML inference execution to more powerful computing devices risks not leveraging on-device capabilities due to additional network latency and connectivity dependency, forgoing the benefits of increased energy efficiency and responsiveness of on-device inference.

In this context, Hierarchical Inference (HI) [25] has recently emerged as a novel distributed ML inference technique that mitigates the limitations of on-device inference by using remote inference when necessary. Under a HI system, inference is performed first on the local DL model for each data sample. A data sample for which the local inference is likely correct is a *simple data sample*, and its inference is accepted, while a data sample for which the local inference is likely incorrect is a *complex data sample*, which is offloaded. By only offloading the complex samples, HI reaps the benefits of performing inference on end devices without compromising on accuracy, and thus, it received considerable attention in the recent past [1, 4, 5, 25, 26].

HI operates through a decision algorithm that acts on the on-device (local ML) model output for each input sample and decides whether to accept the local inference or offload the sample. Consequently, HI requires on-device inference for every sample, introducing a fixed overhead to latency and energy consumption per inference. However, all the existing work on HI only studied

the accuracy improvement over the on-device inference without accounting for its latency and on-device energy consumption overheads. Further, their conclusions were based only on simulations using abstract costs for offloading and misclassification errors. Additionally, they ignore the diversity and heterogeneity of edge ML systems, including varying hardware, network connectivity, and models.

In this paper, we address the above shortcomings and make multiple contributions. We perform accuracy, latency, and energy measurements for running embedded DL models on five devices with different capabilities and three image classification datasets (please refer to Section 3 for additional details about the devices and models used). These measurements will be of independent interest to the embedded ML community. Using the measurements, we empirically evaluate the performance of HI and on-device inference and demonstrate that HI improves accuracy but has higher latency and energy consumption. This raises the question of the true benefits of using HI. We answer this question in light of QoS requirements. We demonstrate that a HI system achieves a given accuracy requirement using a small on-device model, even if this model’s accuracy is below the specified requirement. Consequently, the HI system using the small model achieves lower latency and energy consumption than a larger on-device model that meets the initial accuracy requirement. This establishes the benefit of using HI over on-device inference. For instance, on the Raspberry Pi, with an accuracy requirement of 90% for CIFAR-10 image classification, we demonstrate that using a smaller model, ResNet-8, with HI achieves 95.9% accuracy and has 73% lower latency and 77% lower energy consumption than the on-device larger model, ResNet-56, with 93.7% accuracy. Additionally, HI achieves up to 11% (absolute difference) higher accuracy for a given latency and energy requirement for the systems we studied.

However, for ImageNet-1K image classification, offloading for remote inference remains the only viable solution on Coral Micro and Raspberry Pi due to the lack of on-device models that can provide the necessary lower latency and energy consumption. To alleviate this issue, we resort to the early exit technique [34], which improves HI by reducing the latency of the on-device inference. Using this technique, we design a hybrid system, Early Exit with HI (EE-HI), and demonstrate that compared to HI, EE-HI reduces the latency up to 59.7% and the device’s energy consumption up to 60.4%.

The rest of the paper is organized as follows. In Section 2, we discuss the existing edge ML inference strategies and the related work. In Section 3, we describe the system methodology used for measurements. We present the measurement results and compare the performance of HI, on-device, and remote inference in Section 4. We present the design and the results of EE-HI in Section 5 and conclude in Section 6.

2 EXISTING STRATEGIES FOR EDGE ML INFERENCE

In this section, we discuss the related works in edge ML inference systems. The methods that use on-device inference can be broadly classified into 1) inference load balancing, 2) DNN partitioning, 3) on-device inference, and 4) HI. In the following, an *inference*

¹We focus on image classification datasets and models as they span a broad range of complexity and are widely used benchmarks for evaluating the performance of DL systems [29].

²This value is motivated by the latency requirement of 100 to 500 ms in real-time computer vision applications such as scene text detection [39], and image captioning [40].

task refers to outputting the inference for a given data sample at the device. For the on-device inference strategy, this task is to run the local DL model on the data sample. For remote ML, this task involves offloading the data sample for remote ML inference and receiving the results. The HI this task involves using standalone on-device inference or on-device in conjunction with remote inference based on the HI offloading decision.

Inference Load Balancing: Since the initial proposal of edge computing [32], significant attention has been devoted to the computational offloading for generic compute-intensive applications [23]. Due to the growing importance of edge intelligence, recent studies have examined computation offloading for applications using ML inference [12, 27, 36]. This line of research aims to load-balance the inference task by partitioning the data samples between the device and the server, considering parameters such as job execution times, communication times, energy consumption, and average test accuracy of ML models. However, in [1], Ghina et al. demonstrated that load-balancing data samples may lead to adversarial scenarios where most data samples scheduled on the device receive incorrect inferences. HI circumvents this issue by utilizing the local DL output and offloading a data sample if its local inference is likely incorrect.

DNN Partitioning: DNN partitioning, proposed in [17], partitions the layers of a large-size DL model and deploys the front layers on the mobile device while the deep layers are deployed on an edge server. It received considerable attention recently [14, 21]. However, as demonstrated in [1], for DNN partitioning to be beneficial in reducing the execution time per inference, the processing times of the DL layers on the mobile device should be small relative to the communication time of the data generated between layers. Thus, this technique requires mobile GPUs, making it infeasible for resource-constrained end devices such as IoT devices.

On-Device Inference: As discussed in Section 1, considerable effort has been dedicated to the design of compact DL models tailored for deployment on end devices [6, 10, 30]. Further, techniques such as early exit [34] have been explored to reduce the execution time of DL inference. As a result, state-of-the-art compact DL models can perform simple ML inference tasks on devices, ranging from face recognition on mobile phones [19] to visual wake word and keyword spotting on IoT devices [2]. However, the main focus in designing these models has been improving accuracy, while time per inference and energy consumption have not been critically studied.

To understand the different efficiency aspects of ML models, their performance is required to be measured. However, the complexity of measuring ML performance on resource-constrained devices is challenging. To alleviate such a challenge, an ML performance (MLPerf) benchmarking organization has recently proposed a benchmarking suite, TinyMLPerf, for TinyML models to perform simple inference tasks [2]. Throughput and latency measurements were presented in [35] for ResNet-50 and MobileNet on Jetson Nano and Coral Micro. More fine-grained and precise profiling on Android devices has been proposed by Chu et al. [7], who present nnPerf, a profiler for TensorFlow Lite models. However, none of the above works provide energy measurements or compare edge ML strategies.

Hierarchical Inference: The key to implementing HI is the HI decision module/algorithm for differentiating simple and complex

samples and making the offloading decision. To this end, all existing works use the soft-max value (confidence) output by the local DL model corresponding to each class. An image is classified into the class that has the maximum soft-max value. Nikoloska and Zlatanov [26] computed the HI offloading decision by computing a threshold for the maximum soft-max value based on the transmission energy constraint of the device. Al-Atat et al. [1] proposed a general definition for HI, presented multiple use cases, and compared HI with existing distributed DL inference approaches at the edge. Similar to [26], a threshold was computed based on the trade-off between local misclassifications and offloading costs. Behera et al. [4] showed that using a binary LR on the first two highest soft-max values can improve the HI offloading decision. The binary LR is trained to learn which images are correctly classified and which are incorrectly classified by the local DL. This paper uses the binary LR as the HI decision algorithm. All the above works, however, use simulation to evaluate their performance against on-device inference using abstract costs for offloading and misclassification errors.

2.1 Early Exit with Hierarchical Inference

As stated in Section 1, lower-latency on-device models are necessary for HI implementation. Toward this end, we propose the EE-HI system by combining the HI system with the proven inference acceleration technique early exit [34]. To this end, we modify the base models by adding early exit branches to create new local ML models. This allows for inferences to be accepted early based on the likelihood of the data sample being a simple sample. After the data samples are processed by the early exit local ML, HI is applied on top of it. A binary LR model decides if the local inference (at the final layer) for each data sample suffices or if it needs to be offloaded to the remote server for further inference. This method provides a dynamic and adaptive approach to handling a variety of samples efficiently, optimizing both time and resource utilization. More details of this method are presented in Section 5.

3 SYSTEM AND METHODOLOGY

3.1 Devices

In this study, we conduct measurements on five devices shown in Fig. 2 and described in Tables 1 and 2.

Arduino Nano and ESP32. Arduino Nano 33 BLE Sense and ESP32 (cf. Table 1) are the least powerful devices used in this paper. On-device inference is performed using the TensorFlow Lite Micro framework, which requires loading the model as a binary file, leading to slower on-device computation. Furthermore, contrary to all other devices, it does not support Wi-fi communication. For this reason, in case of offload, the images are transmitted to the edge server via Bluetooth Low Energy (BLE).

Coral Micro. Coral Dev Board Micro (cf. Table 1) possesses higher processing power and more memory than other commodity MCUs, it can load and execute large compute-intensive DL models with higher inference accuracy. Although the device has beneficial features, in certain cases, it falls short. For example, the built-in TPU

supports a limited set of instructions³ that directly impacts the models it can execute. The TFLite models must be compiled using `edgetpu-compiler` to support the built-in TPU. However, because early-exit models use an intermediate layer with an `if` instruction, they cannot be compiled to a model supported by the TPU because the instruction is not supported. One potential mitigation of such an issue is running the model on the CPU at the expense of increased inference latency and energy consumption.

Raspberry Pi 4B. Contrary to Jetson Orin or Coral Micro, the Raspberry Pi 4B (cf. Table 2) does not benefit from any hardware accelerator. Such selection provides us with a broader view of the available system-on-chip ecosystem.

Regarding the software implementation, all the models are loaded and run using the TFLite Python API. All the necessary operations for the tested models are supported in this framework⁴. This, combined with the fact that models were run on the CPU, allows for a smooth deployment even for Early Exit implementations.

Jetson Orin. Jetson Orin Nano (cf. Table 2) includes an integrated GPU that features Tensor Cores. For this device, we have used TensorRT SDK⁵, which is a framework developed by NVIDIA for high-performance deep learning inference, built on top of CUDA. It optimizes the models using layer and tensor fusion and kernel tuning to maximize performance on the specific hardware of the target device. To port the pre-trained models to TensorRT, we must first convert them to ONNX. This pipeline yields correct results for base models, but for early exit we find that the TensorRT engine fails to produce a graph-capturable network in CUDA, which causes early exit models to be slower than the base implementations. To mitigate this issue, transforming the Tensorflow subgraph models to PyTorch successfully generates models that effectively utilize CUDA graphs and achieve the required performance.

Jetson Orin has two power modes: one for maximum performance (15W) with all hardware and clocks at full capacity and another for low power consumption (7W) with RAM, CPU, GPU, and other components capped. We examine both power modes to investigate their effects and observe that enabling dynamic clock rate results in higher latency and variability for relatively small energy savings. Setting the clock to maximum in each power mode results in higher performance per watt and more stable outcomes under constant load.

3.2 Datasets, Models and Training

We study image classification tasks using three datasets MNIST, CIFAR-10, and ImageNet-1K. As discussed in Section 1, MNIST image classification tasks can be performed on Arduino Nano and ESP32, without offloading to a remote ML. Thus, the results for CIFAR-10 and ImageNet-1K image classification tasks are presented in the rest of the paper.

We use TensorFlow⁶ as the DL software library for most of this work due to its popularity and convenience in compiling models

for on-device deployment, thanks to TFLite⁷ and TFLite Micro⁸. We refer to the models we introduce below as *base models* to differentiate them from the models we design and train using early exit branches, later in Section 5.

CIFAR-10. Three models are selected for this dataset. The smallest one being an implementation of ResNet-8 presented by MLPPerf⁹. Another model from the ResNet [13] family is selected as an alternative: ResNet-56. In this case, we trained the model, achieving an accuracy of up to 93.77%. Due to its popularity, AlexNet [18] is also considered in this work. We trained the model up to 74.51% accuracy.

ImageNet-1K. For ImageNet, we select ResNet-18, ResNet-50, AlexNet, and RegNetY32GF [28]. All these models are retrieved from PyTorch’s own model repository¹⁰. Nonetheless, in an attempt to facilitate deployment and preserve framework uniformity, these models are converted to TensorFlow, maintaining the same structure and accuracy.

Early Exit (EE) models. For CIFAR-10 models (ResNet-8, ResNet-56, AlexNet), we design early exit models by implementing the methodology presented in [34]. Our approach differs by placing the threshold on the model confidence, i.e., the highest softmax value, instead of the entropy of all the softmax values.

Early exit model implementation follows a two step process. Firstly, a model with the desired architecture is created by adding branches to the original one, which then becomes the backbone of the new model. It possesses one input and as many outputs as branches selected during the design phase (backbone exit also needs to be considered). This model is trained with a joint loss function obtained via a weighted sum over the individual loss functions of each exit. Once the model is successfully trained, the second step involves adding conditional statements for each branch, such that the new model only has one output.

3.3 Performance Metrics and QoS

We measure the performance of on-device inference, HI, EE-HI, and remote inference strategies using the following three key metrics commonly employed in QoS requirements in edge ML applications¹¹. Each metric is defined as the average over the set of data samples from a dataset.

- **Energy per Inference (EPI):** It refers to the average energy consumed by the device during an inference task¹².
- **Latency per Inference (LPI):** It is the average time taken to process an inference task.
- **Accuracy:** It is the percentage of correct inferences (top-1 accuracy) provided for the validation dataset.

Given different datasets with varying inference task complexity, choosing QoS metrics is non-trivial because the range of accuracy values achieved in edge ML systems is limited by the availability of on-device and remote DL models, which depend on the datasets.

⁷<https://www.tensorflow.org/lite>

⁸<https://www.tensorflow.org/lite/microcontrollers>

⁹<https://github.com/mlcommons/tiny>

¹⁰<https://pytorch.org/vision/stable/models.html>

¹¹<https://mlcommons.org/benchmarks/inference-tiny/>

¹²We only consider the on-device energy consumption, taking into account that devices can be battery limited.

³<https://coral.ai/docs/edgetpu/models-intro/#supported-operations>

⁴https://www.tensorflow.org/mlir/tfl_ops

⁵<https://docs.nvidia.com/deeplearning/tensorrt>

⁶<https://www.tensorflow.org/>

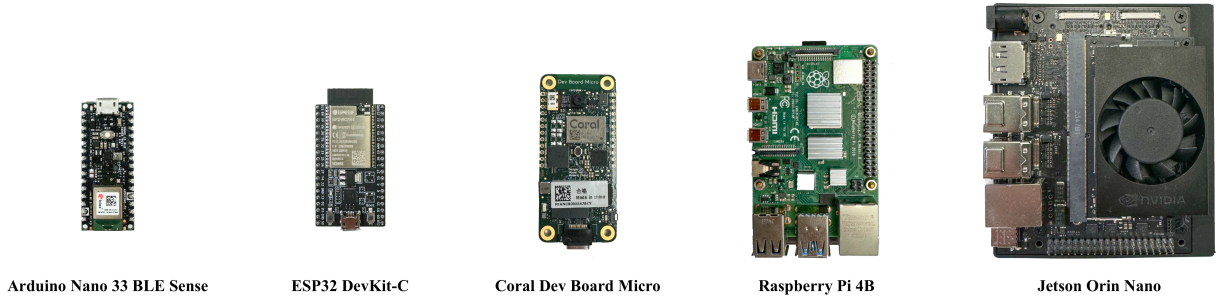


Figure 2: Devices used in the study. Starting from the left: Arduino Nano 33 BLE Sense, ESP32 DevKit-C, Coral Dev Board Micro, Raspberry Pi 4B, Jetson Orin Nano.

Table 1: Device characteristics of MCUs used for the measurements

	ESP32 DevKit-C	Arduino Nano 33 BLE Sense	Coral Dev Board Micro
CPU	Tensilica Xtensa LX6 Dual-Core @ 240 MHz, 160 MHz or 80 MHz	Nordic nRF52840 ARM Cortex-M4 CPU @ 64 MHz	ARMv7 Cortex-M7 @ 800 MHz / M4 @ 400 MHz
Memory	520KB SRAM + 8 KB RTC FAST + 8 KB RTC SLOW	256KB SRAM	64MB RAM
Accelerator	-	-	Coral Edge TPU
Connectivity	Wi-Fi 802.11 b/g/n, Bluetooth v4.2 BR/EDR and BLE	5.0 BLE	Wi-Fi 802.11 a/b/g/n/ac, Bluetooth 5.0 add-on board)

Table 2: Device characteristics of the moderately powerful devices used for the measurements

	Jetson Orin Nano	Raspberry Pi 4B
CPU	ARMv8.2 Cortex-A78AE @ 1.5 GHz	ARMv8 Cortex-A72 @ 1.5GHz
Memory	8GB 128-bit LPDDR5-2133	8GB LPDDR4-3200
Accelerator	Ampere GPU: 1024 CUDA cores + 32 Tensor cores	-
Connectivity	Gigabit Ethernet, 2.4GHz and 5GHz IEEE 802.11.b/g/n/ac wireless, Bluetooth 5.0	Gigabit Ethernet, 802.11ac Wi-Fi, Bluetooth 5.0

Given this difficulty, we choose the following QoS requirements with some justifications.

Minimum accuracy constraint: The accuracy QoS requirement for MNIST and CIFAR-10 image classification is to achieve at 90%, and for ImageNet-1K is to achieve at least 80%. Motivated by [37], we choose the accuracy requirements 10% lower than the state-of-the-art (SOTA) model accuracy for the respective datasets, 99.8% for MNIST [24], 99.5% for CIFAR-10 [11], and 90% for ImageNet-1K [9]).

Maximum latency and energy constraints: The latency QoS requirement is to achieve less than half the time required to offload an image and receive the inference back at the device. The energy QoS requirement is to consume less than half the energy required to offload an image and receive the inference result back at the device.

Note that if latency or energy constraints are relaxed enough to permit offloading an image, remote inference is the best strategy as it achieves higher accuracy. When comparing different strategies in Section 4.4, we fix one of the QoS requirements and determine

the strategy that provides the maximum gains for the other two metrics.

3.4 Methodology for Measurements

3.4.1 On-device. All the models examined in this work are either pre-trained by the authors or obtained from existing libraries. Given that INT8 quantized models have lower latency and energy consumption [15], we build and use quantized models albeit at the expense of slightly lower accuracy than the full-precision models. For each device, we load a pre-trained model and measure its latency and energy consumption by performing inference on n images. The averages are then computed, with n varying according to the size of the dataset. Note that, for the inference evaluation, we measure the latency and energy consumption of the API call that initiates the inference routine in each framework.

The power consumption measurements are performed through a Voltech PM1000+ Power Analyzer and its Universal Breakout Box, which allows devices to be plugged directly into a socket to obtain results. Since the Voltech PM1000+ relies on legacy software, we

created a custom script to issue remote commands to the power analyzer using the PyVISA¹³ library. We obtain the energy values from the average power consumption and the time taken by the underlying inference time or offloading time measurements for inference time and energy consumption for each model. The measurements have a negligible standard deviation. For all the measurements reported in this section, the maximum standard deviation occurred for the power measurement of running AlexNet on Coral Micro, and its value is 6.1% of the mean value.

3.4.2 HI. For the HI system, we choose ResNet-8 and ResNet-18 as the local DL models for CIFAR-10 and ImageNet-1K datasets, as both these models are state-of-the-art tinyML models with a reasonable accuracy-to-size ratio. We also train binary LR models (cf. Section 2) for both datasets. Once the inference is performed on the local DL model for each image, its soft-max values are input to the binary LR. The inference is accepted if the binary LR outputs 1; otherwise, the image is offloaded for remote inference. If the image is set to be offloaded, this is transmitted via the local WiFi network to the edge server. Once the image is fully received on the server, it is preprocessed to the required format of the server model. The server runs the prediction and sends the predicted class back to the device via the network. Given this workflow, the HI system’s accuracy is obtained using (1), where for i -th image, LR_i denotes the result of the binary LR, dev_inf_i and ser_inf_i denote the device and server predictions, gt_i denotes the ground truth class, and N is the size of the test/validation dataset.

$$Acc_{HI} = \frac{\sum_{i=1}^N \mathbb{1}(LR_i=1) \mathbb{1}(dev_inf_i=gt_i) + \mathbb{1}(LR_i=0) \mathbb{1}(ser_inf_i=gt_i)}{N} \quad (1)$$

Alternatively the accuracy of the HI system can also be represented as

$$Acc_{HI} = (Acc_{OD} - \eta_{FN}) + (Acc_S * \eta_{off}) \quad (2)$$

where the accuracy obtained by the on-device and remote inference are denoted as Acc_{OD} and Acc_S respectively. η_{FN} and η_{off} represent the fraction of false negative (FN) samples from the binary LR and the fraction of offloaded samples. It can be inferred from Eq. 2, for a given accuracy QoS, it is important to note that the on-device accuracy does not need to exceed the QoS. The overall system accuracy Acc_{HI} tends to increase with a higher η_{off} , though this improvement comes at the cost of increased latency and energy consumption. Conversely, the Acc_{HI} decreases as η_{FN} increases.

A modular approach was followed for latency and energy measurements for HI. The latency per inference for any image includes the time taken for local DL inference and binary LR decision. If the decision is to offload the image, then the latency accounts for the additional term t_{off} , which is the total time taken for image transmission to the server, remote ML inference, and sending back the prediction to the device. Thus, the average latency under HI is given in 3, where η_{off} is the fraction of offloaded samples. Similarly, the average on-device energy consumption per image is given in (4), where e_{edge_off} is the energy consumed to obtain the remote inference for an offloaded image.

$$Time_{HI} = t_{dev_inf} + t_{LR} + \eta_{off} [t_{off}] \quad (3)$$

$$Energy_{HI} = e_{dev_inf} + e_{LR} + \eta_{off} [e_{edge_off}] \quad (4)$$

3.4.3 EE-HI. For HI system with early exit local DL models, the accuracy, latency, and energy can be computed using (1), (3), and (4). However, in this case, the average latency t_{device_inf} and the energy consumption e_{dev_inf} of the early exit DL model depend on the chosen threshold(s) θ at the early exit branch(s). If the inference of an image satisfies the threshold condition at an early exit branch, then t_{dev_inf} and e_{dev_inf} will only include the processing till that branch.

4 MEASUREMENT RESULTS AND PERFORMANCE COMPARISON

4.1 Server Run times

We measure the run times of the remote ML inference on two distinct servers with different GPUs: NVIDIA Tesla T4 and NVIDIA A100. For CIFAR-10, we consider a pre-trained vision transformer model ViT-H/14 [11], which we fine-tune up to 98.77% accuracy. For ImageNet-1K, we consider a ConvNeXT [22] with 86.58% accuracy. For the former, we measure an average time per inference of 19.18 ms for ViT-H/14 (CIFAR-10) and 12.01 ms for ConvNeXT (ImageNet-1K). For the latter, the measured times are 4.29 ms for ViT-H/14 (CIFAR-10) and 4.41 ms for ConvNext (ImageNet-1K). These numbers are obtained using half-precision (FP16), a format that uses 16 bits to represent floating-point numbers. Both GPUs have specialized hardware for FP16 arithmetic, which increases performance with negligible accuracy loss. Upon arrival, the image needs to undergo a series of manipulations before it can be passed to the model. Including the entire process, the recorded average time for completion of an inference request becomes 6.95 ms for CIFAR-10 and 5.08 ms for ImageNet-1K. The reason for this is that ConvNeXT uses the same input as the edge models. Therefore, when the image is received by the server, we can immediately perform preprocessing, which takes an average of 0.7 ms. However, preparing data for ViT-H/14 is more involved as it entails the transposition of the input buffer to NCHW format and upscaling to the appropriate dimensions before we can proceed with preprocessing. The additional operations are accountable for the uneven increase in the total execution time compared to ConvNeXT.

Considering that both devices are equipped with NVIDIA hardware, TensorRT is deemed the optimal choice for conducting inference testing. Nonetheless, the size of ViT-H/14 exceeds the 2 GB restriction in the Protobuf (Protocol Buffers) serialized message size¹⁴, rendering it impossible to parse the model into the framework. Instead, the ONNX Runtime was utilized with the CUDA execution provider, given that TensorRT execution provider naturally fails in this framework for the same reason. However, the ConvNeXT model did not have this issue, and the inference was executed using TensorRT execution provider within ONNX Runtime.

Given that the runtimes on A-100 are shorter, we use it to offload the images for HI and remote-inference systems.

4.2 Wireless Communication Timings

4.2.1 Image transmission: WiFi vs BLE. Given the availability of both BLE and Wi-Fi for all the devices (except Arduino Nano), the

¹³<https://pyvisa.readthedocs.io/en/latest/>

¹⁴<https://protobuf.dev/programming-guides/encoding/>

Table 3: Latency and energy consumption to offload an image using WiFi.

		Coral	RPi	Jetson	
				7W	15W
CIFAR-10	Latency (ms)	10.37	9.68	8.34	8.20
	Energy (mJ)	14.61	27.67	50.48	55.91
ImageNet-1K	Latency (ms)	84.41	28.74	16.42	16.45
	Energy (mJ)	145.13	112.01	111.57	124.93

question of which one should be used arises. To address this, an experiment was performed on a Raspberry Pi, where both latency and energy were measured for transmitting a CIFAR-10 image to the server and waiting for a response. It is worth noting that the energy measurements were taken for the whole working device, not only the communication module.

As expected, BLE’s power consumption is smaller, 2.23 W, compared to WiFi, which consumes 2.71 W. However, the transmission time of an image under BLE is 177.13 ms, two orders of magnitude higher than the 2.65 ms time it takes for WiFi. Thus, the average energy consumption for transmitting an image to the server and receiving two bytes back consumes 7.39 mJ in the case of Wi-Fi and 395 mJ in the case of BLE. Given significantly high latency and energy consumption under BLE, we opt for Wi-Fi communication for offloading the images.

4.2.2 Measuring offloading time over WiFi. We measure the total time and on-device energy consumption for transmitting an image over Wi-Fi and getting the inference back at the device. The device, operating as a client, transmits a request to the server that is actively monitoring communications. To establish Wi-Fi connectivity, the client connects to a hotspot that access the local network where the server is operating. The experiment was designed to transmit an image as a raw byte array via TCP and receive a number representing the anticipated class by performing inference using the remote ML on the server using the incoming array. The duration between the initiation of the offload process and the reception of the response is repeated and averaged over 10000 images. Measurements for this process with both datasets are presented in Table 3.

4.3 Device Results

The results for base models were acquired on 3 devices (Coral Micro, Raspberry Pi, Jetson Orin) are shown in Table 4. The results for Coral Micro illustrate that for CIFAR-10, AlexNet is inferior to ResNet models in all performance metrics. For ImageNet-1K, the AlexNet model we trained, cannot be loaded on the device due to its size, even when modifying the board’s memory regions via the linker script, in order to allocate more space for it. For the Raspberry Pi, all the models from Subsection 3.2 were successfully run on the device. For Jetson Orin, an important observation is that operating at 15W results in lower energy consumption than 7W power. This is because, at high power, the latency is lower. This observation is akin to BLE vs WiFi offloading time.

Regarding CIFAR-10, Jetson Orin is the most efficient in terms of both energy and latency when compared to the other two devices. However, for Raspberry Pi, the tradeoff is the power efficiency,

which is not as efficient as Coral Micro for ResNet-8 ($\times 2.9$) and ResNet-56 ($\times 5.6$). However, one anomaly is Alexnet, which works significantly more efficient on Raspberry Pi ($\times 5.8$) than on Coral Micro.

For ImageNet-1K, a similar pattern is observed. Yet, when it comes to latency, Raspberry Pi surpasses Coral Micro for ResNet-50 by a factor of 1.5. This indicates that running more complex models on Coral Micro results in additional processing time, even with the assistance of a TPU accelerator.

4.4 On-Device vs. HI vs. Remote Inference

In Fig. 3, we present the accuracy achieved by different strategies for CIFAR-10 and ImageNet-1K datasets, respectively. We present the latency and energy consumption of these strategies on Coral Micro, Raspberry Pi, and Jetson Orin in Figs. 4 and Fig. 5, respectively. ResNet-8 and ResNet-18 are the SOTA tinyML models for CIFAR-10 and ImageNet-1K, respectively, and are used as the local DL models for the HI system. From Figs. 4, and 5, we observe similar trends across the CIFAR-10 and ImageNet-1K datasets for both Coral Micro and Raspberry Pi. In all the subfigures, the smallest local ML models, ResNet-8 for CIFAR-10 and ResNet-18 for ImageNet-1K, consume the least energy and have the lowest latency among the models. However, these models also have the lowest accuracies (cf. Fig. 3) and do not satisfy the accuracy QoS requirements.

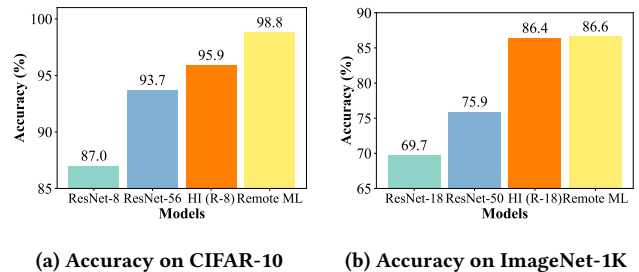


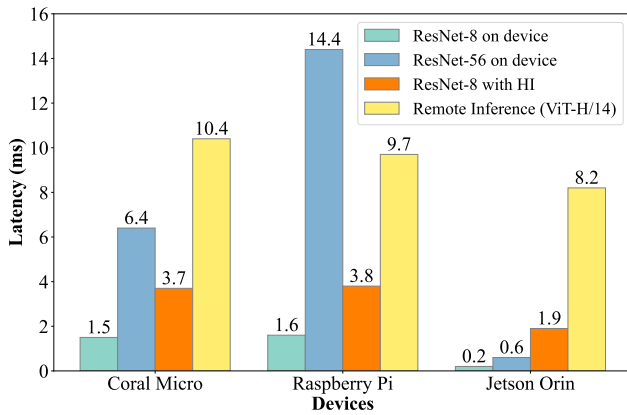
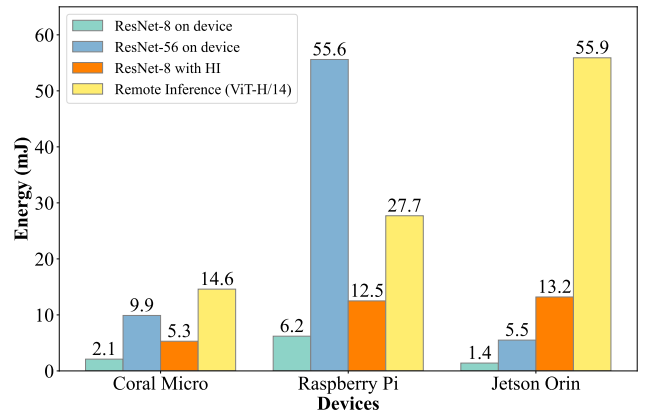
Figure 3: Accuracy of different strategies on CIFAR-10 and ImageNet-1K datasets

The HI system provides better accuracy—up to 2.2% higher for CIFAR-10 (cf. Fig. 3a) and 11.5% higher for ImageNet-1K (cf. Fig. 3b) than both on-device models. This comes with only a slight increase in latency and energy compared to the smallest model (cf. Figs. 4 and 5). Remote ML inference, while yielding the highest accuracy, for CIFAR-10 results in significantly higher latency and energy consumption on both Coral Micro and Raspberry Pi, as shown in Figs. 4a and 4b. However, for ImageNet-1K, offloading the data for remote ML inference results in lower energy consumption and latency due to the increase in the local ML model size and dataset complexity (cf. Figs. 5a, and 5b). In contrast, Jetson Orin, with its GPU acceleration, is highly suitable for on-device inference, as larger models like ResNet-56 for CIFAR-10 and ResNet-50 for ImageNet consume significantly less latency and energy compared to remote ML inference (cf. Figs. 4, and 5).

Next, we compare the performances of three different systems: on-device inference, HI system, and remote inference, based on the QoS requirements defined in Section 3.3. For Arduino Nano and

Table 4: Accuracy, latency and energy results for Coral Micro, Raspberry Pi and Jetson Orin devices

		CIFAR-10			ImageNet-1K		
		ResNet-8	ResNet-56	AlexNet	ResNet-18	ResNet-50	AlexNet
Accuracy (%)	Coral	86.98	93.66	74.39	68.75	74.97	-
	Raspberry	86.97	93.53	74.27	69.67	75.86	56.36
	Jetson 15W	86.91	93.72	74.74	69.59	76.01	56.45
	Jetson 7W	86.91	93.72	74.74	69.59	76.01	56.45
Latency (ms)	Coral	1.50	6.45	69.41	168.22	690.43	-
	Raspberry	1.63	14.36	4.75	227.66	461.84	105.04
	Jetson 15W	0.17	0.64	0.39	0.84	1.80	1.48
	Jetson 7W	0.25	1.03	0.63	1.85	4.04	2.64
Energy (mJ)	Coral	2.14	9.86	112.00	230.68	939.69	-
	Raspberry	6.22	55.59	19.38	977.33	2004.21	446.08
	Jetson 15W	1.38	5.47	4.43	10.56	23.60	22.14
	Jetson 7W	1.72	7.12	5.59	16.13	35.71	27.90

**(a) Latency for CIFAR-10****(b) Energy consumption for CIFAR-10****Figure 4: Latency and energy comparison of on-device and HI systems for CIFAR-10 on different devices.**

ESP32, in Fig. 1 we already showed that doing on-device inference using LR meets the accuracy QoS for the MNIST dataset, with much lower latencies than offloading. However, for CIFAR-10, the SOTA tinyML ResNet-8 fails to meet the 90% QoS requirement, necessitating a larger model. However, high latencies for ResNet-8 on these MCUs suggest even higher latency and energy for larger models, making remote inference the preferred strategy to meet QoS requirements.

For Coral Micro and Raspberry Pi, we observe from Figs. 4a and 4b that, for CIFAR-10 dataset, the on-device ResNet-56 model and the HI system with ResNet-8 can achieve the required accuracy QoS of 90%. Although HI systems add some latency and energy overheads to the on-device model ResNet-8, these are insignificant compared to the much higher latency and energy required for ResNet-56 on-device inference. Consequently, the HI system meets the accuracy QoS with up to 73% lower latency and 77% lesser energy than the on-device model. Given the latency and energy QoS requirements (cf. Table 3) on these two devices, the HI system

achieved more than a 2% absolute accuracy gain. For Jetson Orin, on-device inference using ResNet-56 is much faster and more energy-efficient than the HI system. Thus, for the 90% accuracy requirement, on-device inference suffices. Since the HI system achieves a higher accuracy (1.64% more) while still satisfying the energy and time QoS requirements, HI is the best strategy in those scenarios.

We observe from Table 4 and Fig. 3b that for ImageNet-1K dataset, both the on-device DL models, ResNet-18, and ResNet-50, with accuracies 69.7% and 76%, fall far behind from the required accuracy QoS of 80%. Moreover, both these models demand significantly more energy and latency on Coral Micro and Raspberry Pi compared to remote inference (cf. Figs. 5a and 5b). This makes using even a larger local model in those two devices infeasible. On the other hand, Offloading data samples for remote inference achieves higher accuracy with much lower latency and energy. Hence, remote inference is the best strategy for the 80% accuracy QoS requirement. Further, remote inference is also the fastest and most energy-efficient solution in this scenario.

On Jetson Orin, however, the on-device inference is faster and more energy-efficient. Therefore, we choose the RegNetY32GF

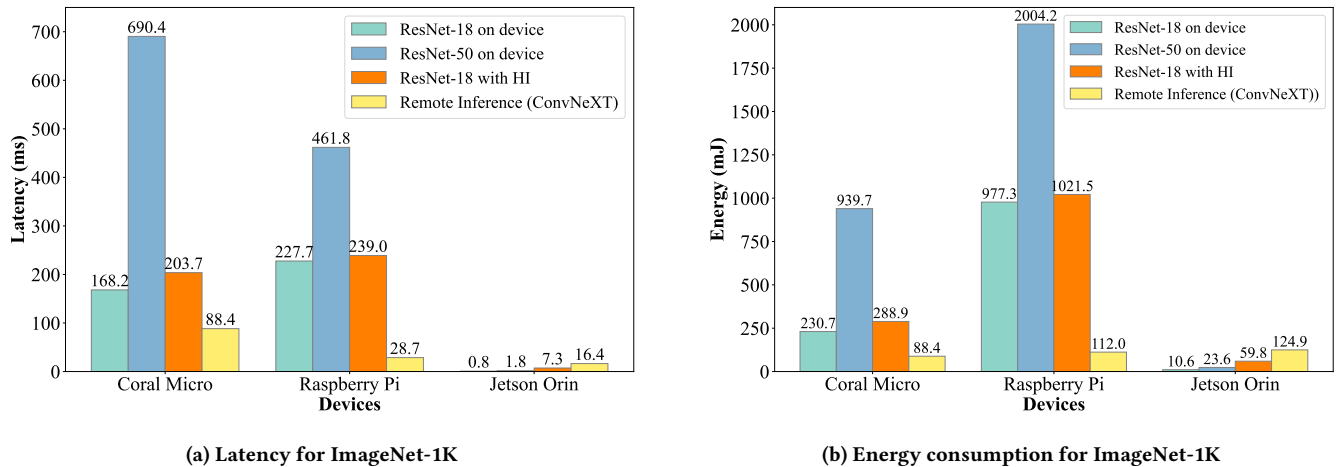


Figure 5: Latency and energy comparison of on-device and HI systems for ImageNet-1K on different devices.

model for on-device inference, as both ResNet-18 and ResNet-50 fail to meet the 80% accuracy requirement. Using RegNetY32GF, we achieved 82.09% accuracy with an inference time of 14.88ms and energy consumption of 213.67mJ, which is higher than that of remote inference. In contrast, the HI system with ResNet-18 meets the accuracy QoS with 50% lower latency and 72% lesser energy. Additionally, HI improves accuracy by 2.14% over RegNetY32GF while satisfying both latency and energy QoS. The best strategies for each QoS requirement are summarized in Table 5.

It is noteworthy that the decision module is crucial to the success of HI systems as demonstrated in Eq. 2. In our experiments, binary LR performed adequately, achieving F1 scores of 0.86 on ResNet-8 for CIFAR-10 and 0.83 on ResNet-18 for the ImageNet-1K dataset. A key insight from the above performance comparison is that:

- In general, for resource-constrained devices, relatively complex tasks (CIFAR-10 for Arduino Nano and ESP32, ImageNet-1K for Coral Micro and Raspberry Pi) require much higher energy and latency to achieve QoS requirements with on-device inference. Consequently, offloading these tasks for remote inference is a better choice.
- If the on-device inference is feasible, it is more beneficial to opt for an HI system with a smaller model that doesn't satisfy the QoS requirement than a larger on-device model that does. HI systems often achieve QoS requirements while optimizing latency and energy consumption (for accuracy QoS and vice versa).

5 EARLY EXIT WITH HI

5.1 Algorithm Description

Equations 3 and 4 show that the latency and energy consumption of a given HI system is a function of four variables: (i) *on-device performance*, (ii) *decision module*, (iii) *offloaded samples ratio*, and (iv) *offload impact*, which includes both the communication cost and the computation cost at the server. Therefore, optimizing any of these variables can enhance the performance of an HI system.

According to inference strategies discussed so far, each sample must pass through the entire local ML model before being either accepted or offloaded. This implies that a fixed latency and energy overhead is added to the system. As existing techniques such as early exit [34] have been shown to reduce on-device overhead while maintaining similar accuracy, we evaluate how introducing this strategy can enhance an HI system. As mentioned earlier, we refer to the case of early exit with HI as EE-HI.

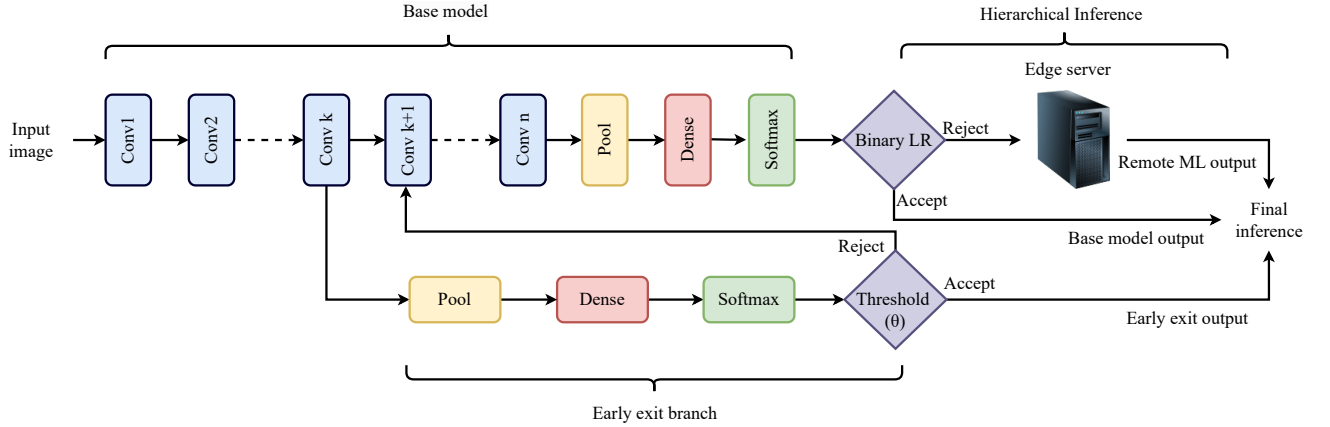
The intuition behind early exit is to create a model capable of assessing how much computation is needed for a given sample. To achieve this, additional branches are attached to the model at different positions, each with its own exit point. During inference, a sample is first evaluated at the initial branch. If the confidence level is sufficient, the system accepts the output and proceeds with the next sample. Otherwise, inference continues to the subsequent branch. Thus, no extra overhead is added unless necessary.

An overview of what an EE-HI system looks like with CNNs is shown in Fig. 6. Several variables need to be considered when designing an early exit architecture, as they significantly impact the performance of the model. Some of the most important variables are the number, placement, and composition of the branches. Nonetheless, selecting these variables is mostly an empirical process, as stated in [20].

The design and training of the models follows the pioneering BranchyNet approach [34] and the training details can be found in Subsection 3.2. We place the branches using a trial-and-error method. For ResNet-8, we use one EE branch after the second residual block or fifth convolutional layer, and for AlexNet, we use one EE branch after the second convolutional layer. For ResNet-56, we use two EE branches, noting that larger models allow for more branches without adding excessive overhead relative to the original latency. The first branch is placed after layer 2, and the second one after layer 19.

Table 5: Preferred strategy for QoS requirements.

Dataset	Device	Best strategy given QoS Requirement		
		Accuracy \geq SOTA -10%	Latency $\leq 0.5 \times$ offload	Energy $\leq 0.5 \times$ offload
CIFAR-10	Coral Micro	ResNet-8 + HI	ResNet-8 + HI	ResNet-8 + HI
CIFAR-10	Raspberry Pi	ResNet-8 + HI	ResNet-8 + HI	ResNet-8 + HI
CIFAR-10	Jetson Orin	On Device (ResNet-56)	ResNet-8 + HI	ResNet-8 + HI
ImageNet-1K	Coral Micro	Remote Inference	Remote Inference	Remote Inference
ImageNet-1K	Raspberry Pi	Remote Inference	Remote Inference	Remote Inference
ImageNet-1K	Jetson Orin	ResNet-18 + HI	ResNet-18 + HI	ResNet-18 + HI


Figure 6: EE-HI for a Convolutional Neural Network (CNN) with a single EE branch.
Table 6: Results for the EE-HI system with optimal threshold subject to the QoS requirement.

Model	Device	Pow.	EE-HI Time (ms)	EE-HI Energy (mJ)	HI Time (ms)	HI Energy (mJ)	EE+HI Threshold
ResNet-8	RaspPi		2.71	9.00	3.82	12.55	$\theta = 0.69$
	Jetson	7W	1.57	9.70	2.04	12.57	
		15W	1.47	10.26	1.87	13.05	
ResNet-56	RaspPi		6.13	23.02	15.21	58.10	$\theta_1 = 0.81$ $\theta_2 = 0.84$
	Jetson	7W	0.84	5.52	1.67	10.95	
		15W	0.69	5.22	1.24	9.63	
AlexNet	RaspPi		5.66	19.47	7.81	28.22	$\theta = 0.75$
	Jetson	7W	2.69	17.12	3.27	21.59	
		15W	2.51	17.98	2.90	21.53	

5.2 Results

In order to compare the performance of this novel strategy, a constraint needs to be set on either accuracy, latency, or energy consumption. This allows us to choose the optimal combination of early exit thresholds that satisfy the given conditions. We adhere to the previously defined minimum accuracy QoS requirement for CIFAR-10, i.e., 90%. We find the optimal threshold combination for each model using a brute-force approach. These results are presented in Table 6, along with those obtained for HI. These experiments are conducted on Raspberry Pi and Jetson Orin using the CIFAR-10 dataset.

It can be seen that in Table 6, for each model and device, EE-HI outperforms the base model with the HI strategy. Reductions of

up to 60% in both latency and energy consumption are observed for ResNet-56 on Raspberry Pi. Fig. 7 provides a more in-depth comparison. For each of the base models, the performance of all the tested strategies is depicted: base model, base model with HI using binary LR (HI), on-device only early exit (EE), EE-HI using binary LR (EE-HI), and remote inference only with a larger ML model (ViT-H/14). For the two early exit strategies, several threshold alternatives are presented, starting from 0.5 and monotonically increasing until a threshold of 1 is reached. Higher thresholds lead to fewer samples being accepted early, resulting in corresponding increments in both accuracy and latency. Consequently, a trade-off between latency/energy and accuracy can be observed. The point where the dotted lines intersect the QoS requirement limit yields the optimal threshold presented in Table 6.

On-device-only EE models (orange dots) fail to achieve the QoS requirement, regardless of the selected threshold. Furthermore, they also fail to reach the base model accuracy except for AlexNet. However, with the appropriate threshold selection, they can lead to notable improvements in terms of latency and energy with reasonable accuracy.

The more branches that are introduced in the model, the more flexibility there is in terms of the accuracy-latency trade-off. This can be observed for ResNet-56 implementations in Fig. 7. The dark-colored lines depict all the possible configurations attainable once

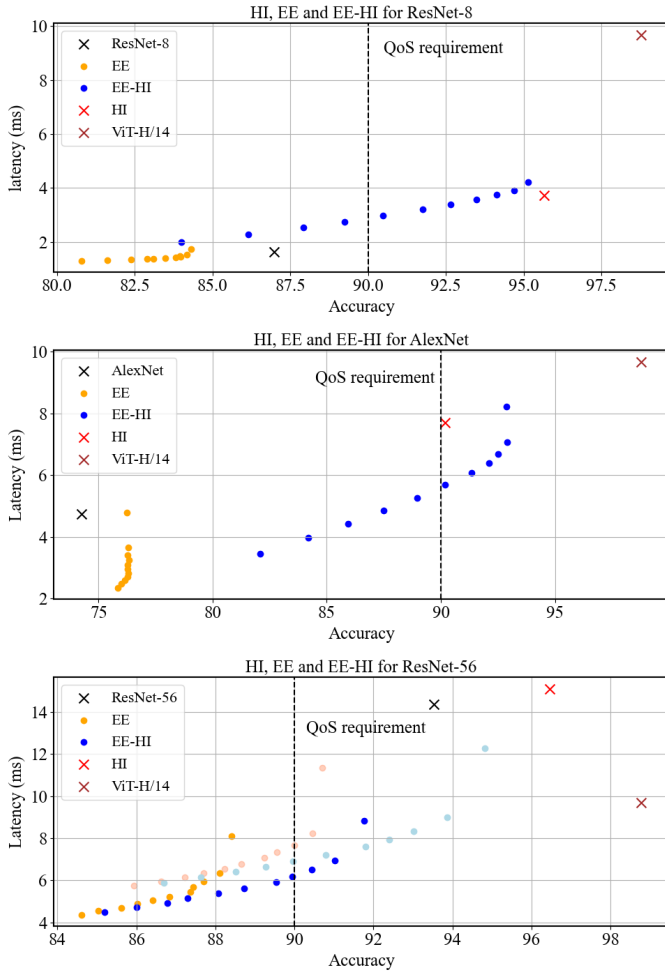


Figure 7: EE, HI, EE-HI comparison for different models for CIFAR-10 on Raspberry Pi.

the first threshold is fixed to $\theta_1 = 0.81$. However, to illustrate the concept, two light-colored lines are presented. These are obtained by fixing $\theta_1 = 0.95$ and varying θ_2 . Although they do not provide the optimal configuration for the given QoS, they can reach much higher accuracy while still benefiting from latency reductions. Consequently, EE-HI emerges as the best strategy under the given circumstances, benefiting from the accuracy boosts of HI and the acceleration of early exit models.

6 CONCLUSION AND FUTURE WORK

In this work, we have empirically demonstrated that the HI system complements the on-device inference by providing up to 73% reduction in latency and 77% reduction in on-device energy consumption in the studied scenarios. Additionally, we have designed a hybrid EE-HI system that features early exits within the HI framework. This approach allows us to achieve up to 60% reduction in latency and energy consumption compared to HI alone for CIFAR-10 image classification on Raspberry Pi and Jetson Orin Nano. Despite these

advancements, using HI remains inferior to remote inference in certain scenarios where no on-device models are small enough to meet latency and energy QoS requirements while maintaining reasonable accuracy. This highlights the need for designing DL models with a better accuracy-to-size ratio than current SOTA on-device models.

Our work opens several new research directions. We used the BranchyNet design approach [34] for early exit technique. Although pioneering, BranchyNet is not the most sophisticated approach. We aim to explore novel techniques like self-distillation [38], which show significant improvement in early exit implementation by reducing latency and energy consumption and improving accuracy compared to the base model. We also plan to investigate how this concept could identify complex samples earlier in the network, further accelerating system inference. While binary LR is an effective HI offloading decision algorithm, it does result in some false positives (correct local inference samples that are offloaded) and false negatives (incorrect local inference samples that are not offloaded). In our HI systems, the binary LR achieved an F1 score of 0.86 for ResNet-8 on CIFAR-10 and an F1 score of 0.83 for ResNet-18 on ImageNet-1K. We aim to explore other HI offloading decision algorithms that further reduce false positives and false negatives, thereby improving the efficiency of HI systems. Additionally, developing local ML models with a high accuracy-to-size ratio will ensure that these models achieve the stringent QoS requirements with HI while maintaining lower latency and energy consumption. Finally, our experiments used a static setup with a dedicated server and stable WiFi access, resulting in consistent offloading times. Studying the effect of device mobility and network interference on the offloading times and the efficiency of HI systems is left for future work.

ACKNOWLEDGEMENT

This work is supported by

- The European Union through Marie Skłodowska-Curie Actions - Postdoctoral Fellowships (MSCA-PF) Project “DIME: Distributed Inference for Energy-efficient Monitoring at the Network Edge” under Grant 101062011 and by the “European Union – Next Generation EU”.
- The Ministry of Employment and Social Economy of Spain through the Spanish Recovery, Transformation and Resilience Plan, in the framework of “Programa Investigo” call.
- MAP-6G (TSI-063000-2021-63) and RISC-6G (TSI-063000-2021-59) granted by the Ministry of Economic Affairs and Digital Transformation and the European Union-Next Generation EU through the UNICO-5G R&D program of the Spanish Recovery, Transformation and Resilience Plan.
- Business Finland project Digital Twinning of Personal Area Networks for Optimized Sensing and Communication (8782/31/2022)

REFERENCES

- [1] Ghina Al-Atat, Andrea Fresa, Adarsh Prasad Behera, Vishnu Narayanan Moothath, James Gross, and Jaya Prakash Champati. 2023. The case for hierarchical deep learning inference at the network edge. In *Proc. Workshop on Networked AI Systems, MobiSys*. 1–6.
- [2] Colby Banbury et al. 2021. MLPerf Tiny Benchmark. *Proc. NeurIPS (Systems Track on Datasets and Benchmarks)* (2021).

- [3] Colby Banbury, Chuteng Zhou, Igor Fedorov, Ramon Matas, Urmish Thakker, Dibakar Gope, Vijay Janapa Reddi, Matthew Mattina, and Paul Whatmough. 2021. Micronets: Neural network architectures for deploying tinyml applications on commodity microcontrollers. *Proceedings of machine learning and systems* 3 (2021), 517–532.
- [4] Adarsh Prasad Behera, Roberto Morabito, Joerg Widmer, and Jaya Prakash Champati. 2023. Improved Decision Module Selection for Hierarchical Inference in Resource-Constrained Edge Devices. In *Proc. ACM Mobicom*. 1–3.
- [5] Hasan Burhan Beytur, Ahmet Gunhan Aydin, Gustavo de Veciana, and Haris Vikalo. 2024. Optimization of Offloading Policies for Accuracy-Delay Tradeoffs in Hierarchical Inference. In *Proc. IEEE INFOCOM (to appear)*.
- [6] Yanjiao Chen, Baolin Zheng, Zihan Zhang, Qian Wang, Chao Shen, and Qian Zhang. 2020. Deep learning on mobile and embedded devices: State-of-the-art, challenges, and future directions. *Comput. Surveys* 53, 4 (2020), 1–37.
- [7] Haolin Chu, Xiaolong Zheng, Liang Liu, and Huadong Ma. 2023. nnPerf: Demystifying DNN Runtime Inference Latency on Mobile Platforms. In *Proc. ACM SenSys*. 125–137.
- [8] Gemma Team (Google DeepMind). 2024. Gemma: Open Models Based on Gemini Research and Technology. arXiv:2403.08295 [cs.CL]
- [9] Mostafa Dehghani, Josip Djolonga, Basil Mustafa, Piotr Padlewski, Jonathan Heek, Justin Gilmer, Andreas Peter Steiner, Mathilde Caron, Robert Geirhos, Ibrahim Alabdulmohsin, et al. 2023. Scaling vision transformers to 22 billion parameters. In *International Conference on Machine Learning*. PMLR, 7480–7512.
- [10] Lei Deng, Guoqi Li, Song Han, Luping Shi, and Yuan Xie. 2020. Model compression and hardware acceleration for neural networks: A comprehensive survey. *Proc. IEEE* 108, 4 (2020), 485–532.
- [11] Alexey Dosovitskiy, Lucas Beyer, Alexander Kolesnikov, Dirk Weissenborn, Xiuhua Zhai, Thomas Unterthiner, Mostafa Dehghani, Matthias Minderer, Georg Heigold, Sylvain Gelly, et al. 2020. An Image is Worth 16x16 Words: Transformers for Image Recognition at Scale. In *proc. ICLR*.
- [12] Andrea Fresa and Jaya Prakash Champati. 2023. Offloading Algorithms for Maximizing Inference Accuracy on Edge Device in an Edge Intelligence System. *IEEE Transactions on Parallel and Distributed Systems* 34, 7 (2023), 2025–2039.
- [13] Kaiming He, Xiangyu Zhang, Shaoqing Ren, and Jian Sun. 2016. Deep residual learning for image recognition. In *Proc. IEEE CVPR*. 770–778.
- [14] Chenghao Hu and Baochun Li. 2022. Distributed Inference with Deep Learning Models across Heterogeneous Edge Devices. In *Proc. IEEE INFOCOM*. 330–339.
- [15] Itay Hubara, Matthieu Courbariaux, Daniel Soudry, Ran El-Yaniv, and Yoshua Bengio. 2018. Quantized neural networks: Training neural networks with low precision weights and activations. *Journal of Machine Learning Research* 18, 187 (2018), 1–30.
- [16] imagimob. 2024. Production grade ML applications on Edge Devices. <https://www.imagimob.com/>. Accessed: date-of-access.
- [17] Yiping Kang, Johann Hauswald, Cao Gao, Austin Rovinski, Trevor Mudge, Jason Mars, and Lingjia Tang. 2017. Neurosurgeon: Collaborative intelligence between the cloud and mobile edge. *ACM SIGARCH Computer Architecture News* 45, 1 (2017), 615–629.
- [18] Alex Krizhevsky, Ilya Sutskever, and Geoffrey E Hinton. 2012. Imagenet classification with deep convolutional neural networks. *Advances in neural information processing systems* 25 (2012).
- [19] Nicholas D Lane, Sourav Bhattacharya, Akhil Mathur, Petko Georgiev, Claudio Forlivesi, and Fahim Kawsar. 2017. Squeezing deep learning into mobile and embedded devices. *IEEE Pervasive Computing* 16, 3 (2017), 82–88.
- [20] Stefanos Laskaridis, Alexandros Kouris, and Nicholas D Lane. 2021. Adaptive inference through early-exit networks: Design, challenges and directions. (2021), 1–6.
- [21] En Li, Liekang Zeng, Zhi Zhou, and Xu Chen. 2020. Edge AI: On-Demand Accelerating Deep Neural Network Inference via Edge Computing. *IEEE Transactions on Wireless Communications* 19, 1 (2020), 447–457.
- [22] Zhuang Liu, Hanzi Mao, Chao-Yuan Wu, Christoph Feichtenhofer, Trevor Darrell, and Saining Xie. 2022. A convnet for the 2020s. In *Proceedings of the IEEE/CVF conference on computer vision and pattern recognition*. 11976–11986.
- [23] Pavel Mach and Zdenek Becvar. 2017. Mobile Edge Computing: A Survey on Architecture and Computation Offloading. *IEEE Communications Surveys Tutorials* 19, 3 (2017), 1628–1656.
- [24] Vittorio Mazzia, Francesco Salvetti, and Marcello Chiaberge. 2021. Efficient-capsnet: Capsule network with self-attention routing. *Scientific reports* 11, 1 (2021), 14634.
- [25] Vishnu Narayanan Moothedath, Jaya Prakash Champati, and James Gross. 2024. Getting the Best Out of Both Worlds: Algorithms for Hierarchical Inference at the Edge. *IEEE Tran. on Machine Learning in Comm. and Netw.* 2 (2024), 280–297.
- [26] Ivana Nikoloska and Nikola Zlatanov. 2021. Data Selection Scheme for Energy Efficient Supervised Learning at IoT Nodes. *IEEE Communications Letters* 25, 3 (2021), 859–863.
- [27] Samuel S. Ogden and Tian Guo. 2020. MDINFERENCE: Balancing Inference Accuracy and Latency for Mobile Applications. In *Proc. IEEE IC2E*. 28–39.
- [28] Ilija Radosavovic, Raj Prateek Kosaraju, Ross Girshick, Kaiming He, and Piotr Dollár. 2020. Designing network design spaces. In *Proceedings of the IEEE/CVF conference on computer vision and pattern recognition*. 10428–10436.
- [29] Vijay Janapa Reddi, Christine Cheng, David Kanter, Peter Mattson, Guenther Schmuelling, Carole-Jean Wu, Brian Anderson, Maximilien Breughe, Mark Charlebois, William Chou, et al. 2020. Mlperf inference benchmark. In *Proc. IEEE ISCA*. IEEE, 446–459.
- [30] Ramon Sanchez-Iborra and Antonio F Skarmeta. 2020. Tinyml-enabled frugal smart objects: Challenges and opportunities. *IEEE Circuits and Systems Magazine* 20, 3 (2020), 4–18.
- [31] Mark Sandler, Andrew Howard, Menglong Zhu, Andrey Zhmoginov, and Liang-Chieh Chen. 2018. Mobilenetv2: Inverted residuals and linear bottlenecks. In *Proc. IEEE CVPR*. 4510–4520.
- [32] Mahadev Satyanarayanan, Paramvir Bahl, Ramón Caceres, and Nigel Davies. 2009. The case for vm-based cloudlets in mobile computing. *IEEE pervasive Computing* 8, 4 (2009), 14–23.
- [33] Mingxing Tan and Quoc Le. 2019. Efficientnet: Rethinking model scaling for convolutional neural networks. In *Proc. ICML*. PMLR, 6105–6114.
- [34] Surat Teerapittayanon, Bradley McDanel, and Hsiang-Tsung Kung. 2016. Branchynet: Fast inference via early exiting from deep neural networks. In *2016 23rd international conference on pattern recognition (ICPR)*. IEEE, 2464–2469.
- [35] Peter Torelli and Mohit Bangale. 2021. Measuring inference performance of machine-learning frameworks on edge-class devices with the MLMark benchmark. <https://www.eembc.org/techlit/articles/MLMARK-WHITEPAPER-FINAL-1.pdf>. *Technical Report* (2021).
- [36] Junjie et al. Wang. 2018. Bandwidth-efficient live video analytics for drones via edge computing. In *Proc. ACM/IEEE SEC*. 159–173.
- [37] Guangyu Wu, Fuhui Zhou, Yuben Qu, Puhuan Luo, and Xiang-Yang Li. 2023. QoS-Ensured Model Optimization for AIoT: A Multi-Scale Reinforcement Learning Approach. *IEEE Transactions on Mobile Computing* (2023).
- [38] Linfeng Zhang, Chenglong Bao, and Kaisheng Ma. 2021. Self-distillation: Towards efficient and compact neural networks. *IEEE Transactions on Pattern Analysis and Machine Intelligence* 44, 8 (2021), 4388–4403.
- [39] Xinyu Zhou, Cong Yao, He Wen, Yuzhi Wang, Shuchang Zhou, Weiran He, and Jiajun Liang. 2017. East: an efficient and accurate scene text detector. In *Proc. IEEE CVPR*. 5551–5560.
- [40] Yuanen Zhou, Yong Zhang, Zhenzhen Hu, and Meng Wang. 2021. Semi-autoregressive transformer for image captioning. In *Proc. IEEE CVF*. 3139–3143.

APPENDIX

6.1 Additional measurements

In Table 7, we present the accuracy and latency measurements taken for Arduino Nano and ESP-32 for CIFAR-10 dataset. As mentioned before, these MCUs possess very limited computational capabilities making it hard to satisfy latency requirements for even moderately complex tasks. The average latency for a single on-device inference is approximately 6.5 times slower than that of remote inference for the Arduino Nano, and nearly 60 times slower for the ESP-32. It should be noted that remote inference is significantly faster on the ESP-32 because it uses Wi-Fi as its communication protocol, as opposed to Bluetooth used by the Arduino Nano. Therefore, the preferred solution would be to offload the inference task to a powerful edge server and receive the corresponding prediction. This offloading process is labeled as "Remote" in Table 7. The term "HI" refers to the entire system, encompassing both on-device inference and remote inference for a specified subset of images, denoted as "% offload," which indicates the percentage of total images that are offloaded for more detailed inference.

In Table 8, we present the latency and accuracy measurements for the base models on the Jetson Orin Nano with different precision levels. The entire test set for CIFAR-10 and the entire validation set for ImageNet-1k have been used for accuracy computation. For latency measurement, the values are averaged over 10000 images, that are randomly selected. This table reinforces the effects of quantization from a precise measurement standpoint. We can observe

Table 7: ResNet-8 on CIFAR-10 results for Arduino Nano and ESP-32.

		Arduino	ESP-32
Accuracy	Device	87.07	
	HI (% offload)	95.75 (21.57)	
Latency (ms)	Device	1230.48	602.52
	Remote	190.35	10.10

that as models are further quantized, the average latency requirements for a single inference reduce gradually without significantly impacting accuracy. Another key observation is that quantization strategies are more beneficial for larger models compared to smaller ones. For example, with the CIFAR-10 dataset, full integer quantization results in a 19% reduction in latency for ResNet-8 compared to full precision. In contrast, ResNet-56 and AlexNet experience

42% and 53% reduction, respectively. For the ImageNet-1K dataset, however, all three models exhibit similar gains in latency reduction, each achieving around 69%.

Table 8: Latency and accuracy for the base models on the Jetson Orin Nano with different precision levels.

		FP32		FP16		INT8		
		Power Mode	15 W	7 W	15 W	7 W	15 W	7 W
CIFAR	Resnet8	Accuracy (%)	87.19		87.16		86.86	
		Latency (ms)	0.212785	0.306191	0.183042	0.260383	0.171250	0.249488
	Resnet56	Accuracy (%)	93.75		93.76		93.65	
		Latency (ms)	1.102070	1.665560	0.762705	1.150450	0.640057	1.035910
	Alexnet	Accuracy (%)	74.52		74.52		74.63	
		Latency (ms)	0.844494	1.759410	0.551228	0.959152	0.389317	0.627006
Imagenet	Resnet18	Accuracy (%)	70		69.812		69.592	
		Latency (ms)	2.74285	6.81942	1.26768	2.81547	0.8375	1.85074
	Resnet50	Accuracy (%)	76.088		76.078		76.010	
		Latency (ms)	5.82106	13.5075	2.8421	6.32683	1.80605	4.03902
	Alexnet	Accuracy (%)	56.544		56.534		56.452	
		Latency (ms)	4.58609	8.41834	2.38455	4.23303	1.47918	2.63732